Folding Control and Unfolding Free Energy of Yeast Iso-1-cytochrome *c* Bound to Layered Zirconium Phosphate Materials Monitored by Surface Plasmon Resonance

Akhilesh Bhambhani,[‡,§] Soonwoo Chah,[†] Eli G. Hvastkovs,[‡] Gary C. Jensen,[‡] James F. Rusling,[‡] Richard N. Zare,[†] and Challa V. Kumar*[,‡]

Department of Chemistry, Stanford University, Stanford, California 94305-5080, and Department of Chemistry, Box U-3060, University of Connecticut, Storrs, Connecticut 06269-3060

Received: December 30, 2007; Revised Manuscript Received: April 30, 2008

The free energy change ($\Delta G°$) for the unfolding of immobilized yeast iso-1-cytochrome *c* (Cyt *c*) at nanoassemblies was measured by surface plasmon resonance (SPR) spectroscopy. Data show that SPR is sensitive to protein conformational changes, and protein solid interface exerts a major influence on bound protein stability. First, Cyt *c* was self-assembled on the Au film via the single thiol of Cys-102. Then, crystalline sheets of layered α-$Zr(O_3POH)_2 \cdot H_2O$ (α-ZrP) or $Zr(O_3PCH_2CH_2COOH)_2 \cdot xH_2O$ (α-ZrCEP) were adsorbed to construct α-ZrP/Cyt *c*/Au or α-ZrCEP/Cyt *c*/Au nanoassemblies. The construction of each layer was monitored by SPR, in real time, and the assemblies were further characterized by atomic force microscopy and electrochemical studies. Thermodynamic stability of the protein nanoassembly was assessed by urea-induced unfolding. Surprisingly, unfolding is reversible in all cases studied here. Stability of Cyt *c* in α-ZrP/Cyt *c*/Au increased by ∼4.3 kJ/mol when compared to the unfolding free energy of Cyt *c*/Au assembly. In contrast, the protein stability decreased by ∼1.5 kJ/mol for α-ZrCEP/Cyt *c*/Au layer. Thus, OH-decorated surfaces stabilized the protein whereas COOH-decorated surfaces destabilized it. These data quantitate the role of specific functional groups of the inorganic layers in controlling bound protein stability.

Introduction

Enzymes and proteins are often immobilized on solid supports for a variety of important practical applications in biosensing and biocatalysis.[1–6] Enhancing the stability of the bound enzyme is a key issue for these and other applications varying from successful development of reusable and stable medical and analytical devices[7,8] to the development of enzyme-based biofuel cells.[9] Therefore, a systematic evaluation of the stability of solid-bound enzymes will be essential to tailor the surface functions of the solid support for maximizing enzyme stability. In this report, the influence of specific functional groups of the support matrix on protein stability is quantitated by a rapid, noninvasive, reversible, and direct method.

We recently demonstrated the use of surface plasmon resonance spectroscopy (SPR) to quantitate $\Delta G°$ of protein unfolding at Au surface.[10] This approach took advantage of the fact that SPR is extremely sensitive to the conformational status of the adsorbed protein film.[11] Urea-induced unfolding of the protein at the Au surface was accompanied by specific changes in the SPR signals, and these are consistent with changes in the refractive index of the medium adjacent to the Au surface.[12] For the first time, SPR changes were used to estimate $\Delta G°$ for protein unfolding, with good precision. For example, $\Delta G°$ for the unfolding of yeast iso-1-cytochrome *c* (Cyt *c*) bound to Au surface was 4-fold lower than that of the free protein, indicating unfavorable interactions with the Au surface.

Here, we demonstrate that this method can be extended to monitor protein unfolding at any desired solid, not limited to Au, and this extension is essential to systematically quantify the influence of specific interfaces on bound-protein stability. In this new approach, the protein is first bound to the Au film; then, the solid of interest is adsorbed onto the protein layer, and the protein conformational status is monitored by SPR. This approach provides a novel, sensitive, noncalorimetric method to directly estimate thermodynamic stability of any protein in contact with a desired solid.

We chose to study Cyt *c* stability at inorganic layered solids, α-Zr^{IV} phosphate (α-ZrP) or α-Zr^{IV} carboxyethyl phosphonate (α-ZrCEP, Chart 1), for multiple reasons. Previously, a general method for the binding of numerous proteins and enzymes to these well-defined layered inorganic solids was developed,[13–15] and bound proteins indicated improved properties, in specific cases.[16–18] For example, Cyt *c*, horseradish peroxidase, met-myoglobin, met-hemoglobin, and lysozyme bind strongly to α-ZrP and α-ZrCEP, under mild, ambient conditions (pH 7, 25 °C).[13]

Enzymes and proteins bound to these solids retained their structure as well as activity to a significant extent, and this is important for applications in biocatalysis.[19,20] Another advantage is that the surface functionalities of these solids can be systematically varied to control enzyme−solid interactions.[21,22] This approach of changing the surface functions of the solid provides a powerful handle to examine how specific functional groups on the solid influence the bound-enzyme stability. Earlier, we demonstrated improved stability of proteins sandwiched in polyion matrixes to extreme pH conditions.[23] Differential scanning calorimetric studies on enzyme/inorganic materials revealed that thermal unfolding is primarily irreversible on the calorimetric time-scales, and hence, the corresponding $\Delta G°$ values for unfolding could not be extracted.[24] This necessitated the invention of the current strategy to quantify $\Delta G°$ for this process, at solid surfaces. Here, we report the thermodynamic

* Corresponding author. E-mail: Challa.Kumar@UCONN.edu. Fax: 860-486-2981.
† Stanford University.
‡ University of Connecticut.
§ Current address: Department of Pharmaceutical Chemistry, University of Kansas, Lawrence Kansas 66047-1620.

10.1021/jp7121642 CCC: $40.75
Published on Web 07/04/2008

CHART 1: (A) Schematic Representation of a Single Layer of α-Zr^{IV} Phosphate, (B) Free OH Groups of Each Phosphate Lying above and below the α-ZrP Plane, and (C) Structure of α-Zr^{IV}Carboxyethyl Phosphonate (α-ZrCEP) That Is Similar to That of α-ZrP Where the OH Groups Are Replaced by CH_2CH_2COOH Functions

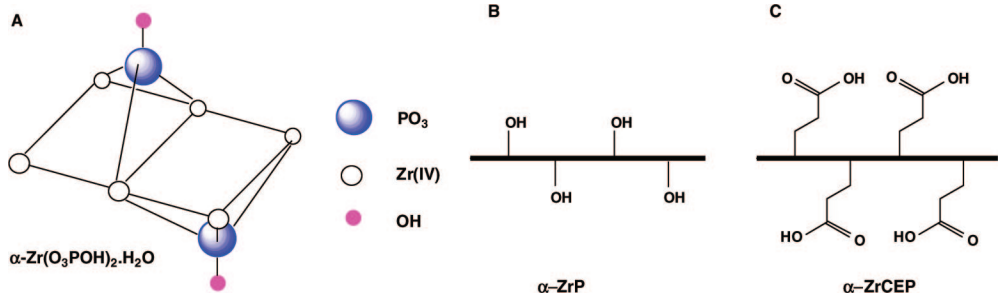

CHART 2: (A) Formation of the Self-Assembled Monolayer of Yeast-Cyt *c* (Filled Circles), (B) Exfoliation of α-ZrP or α-ZrCEP Stacks by Tetrabutylammonium Hydroxide (TBAOH, Open Circles) and Exposure of the Inorganic Plates to Cyt *c* SAM To Construct the Nanoassembly, and (C) Control Experiment Where α-ZrP or α-ZrCEP Was Bound to a Positively Charged, 2-Aminoethane Thiol (AET) SAM, Instead of Cyt *c* SAM

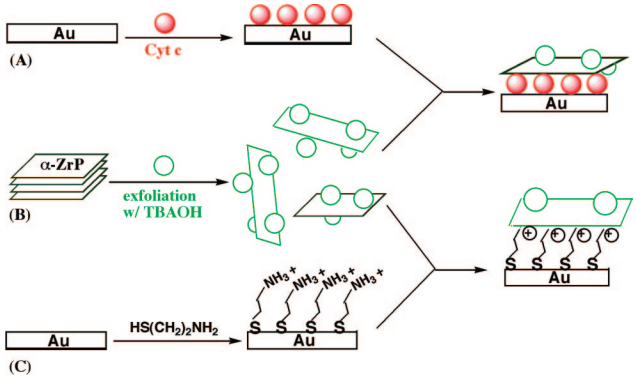

stabilities of Cyt *c* nanoassemblies constructed with inorganic solids (Chart 2). Current results show that specific surface functions of the solid have a significant impact on bound-protein stability.

We chose Cyt *c* for the current studies (pI = 10) because its crystal structure is known, and it binds to Au by forming a Au−thiol bond via the single Cys-102 residue located near the protein surface. Binding to Au causes some distortion of Cyt *c*[25] and the decrease in protein stability, which was quantified recently.[10] Because Cyt *c* has a high affinity for α-ZrP[13] (binding constant is 4.2×10^6 M^{-1}), the SPR method outlined below can be used to measure Cyt *c* stability at inorganic solids.

Our strategy involves the formation of Cyt *c* SAM on an ultrathin Au film (<50 nm), adsorption of the inorganic solid on to the protein SAM (Chart 2), followed by monitoring urea-induced protein unfolding by SPR. This allows the direct monitoring of protein unfolding/refolding in real time, a label-free method, but also provides quantitative estimates of the influence of specific surface groups of the solid on protein stability. Urea-induced unfolding is reversible at the surfaces examined here, and the data indicate significant contributions of the surface functions on Cyt *c* stability.

Experimental Section

Protein Sources. Cyt *c* was purchased from Sigma Chemical Co. (St. Louis, MO), and purity was ascertained to be >99% by SDS PAGE. Protein solutions (35 μM) were made in potassium phosphate buffer (10 mM, pH adjusted to 7.2) unless stated otherwise.

Synthesis of α-ZrP and α-ZrCEP. Zr(IV) phosphate and α-Zirconium carboxyethylphosphonate (α-$Zr(O_3P\ CH_2CH_2COOH)_2 \cdot H_2O$, α-ZrCEP) were prepared as described earlier.[21] The FTIR spectra and the powder XRD patterns of the samples (*d* spacing of 7.6 Å for α-ZrP and 13.1 Å for α-ZrCEP) matched with those reported.[21,26]

SPR. The construction and validation of the SPR instrument, operating in the Kretchmann configuration, was described previously.[10] A brief description of the apparatus follows. The incident light from a 658 nm/30 mW diode laser (LDCU5/4853, Power Technologies, p-polarized) was focused onto the Au substrate, and the intensity of the reflected light was measured by a photodiode (201/579−7227, Thorlabs Inc.) connected to an oscilloscope (TDS640, Tektronix). The glass substrate coated with an ultrathin film of Au was in contact with a right-angled SF10 prism (1.5 cm × 1.5 cm, CVI Laboratories) via index matching fluid ($n = 1.730 \pm 0.0005$, Cargille Laboratories, Inc.). A Teflon cell, with an O-ring of i.d. 0.6 cm, was used to confine the solution in contact with the Au film. Both the prism and the cell were mounted on a goniometer (415, Huber) to control the angle of incidence.(Chart 3).

SPR Substrate Preparation. SF10 glass substrate (3 in × 1 in, Schott Glass Technology) was cleaned, Au film was deposited, and Cyt *c* adsorption was carried out as described earlier.[10] Protein adsorption was monitored by SPR in real time, and the angular dependence of the SPR profiles was matched with the reported curves.[10] Adsorption of the protein was also supported by X-ray photoelectron spectroscopy (Supporting Information, #1).

Subsequent to Cyt *c* self-assembly on Au, the protein layer was exposed to suspensions of α-ZrP (or α-ZrCEP) particles. α-ZrP, or α-ZrCEP, (2%) suspensions were prepared by mixing 0.1 g of α-ZrP (or α-ZrCEP) in 5 mL of distilled water with stoichiometric amounts of tetrabutyl ammonium hydroxide (40% by weight in water).[21,22]Adsorption of the inorganic nanoparticles on the protein layer was monitored by SPR, and the adsorption was further confirmed by energy dispersive X-ray spectroscopy (EDX, Sirion 200, FEI company, Supporting Information, #2).

Atomic Force Microscopy (AFM). Adsorption, surface roughness, and morphology modification was examined by AFM (Digital Instruments Nanoscope IV, operating in the tapping mode). Silicon AFM probes from Veeco Probes (Model no. MPP-11100, symmetric tip, frequency 300 kHz, spring constant 40 N/m) were used. Samples were washed with deionized water and dried with a stream of nitrogen immediately before scanning.

Urea-Induced Unfolding. The protein nanoassemblies were exposed to increasing concentrations of urea (0−7 M in 10 mM

CHART 3: (A) Schematic Diagram of the SPR Setup (Not to Scale), (B) SF10 Glass Slide Coated with a Au Film Attached to a SF10 Prism with Index Matching Fluid.[a]

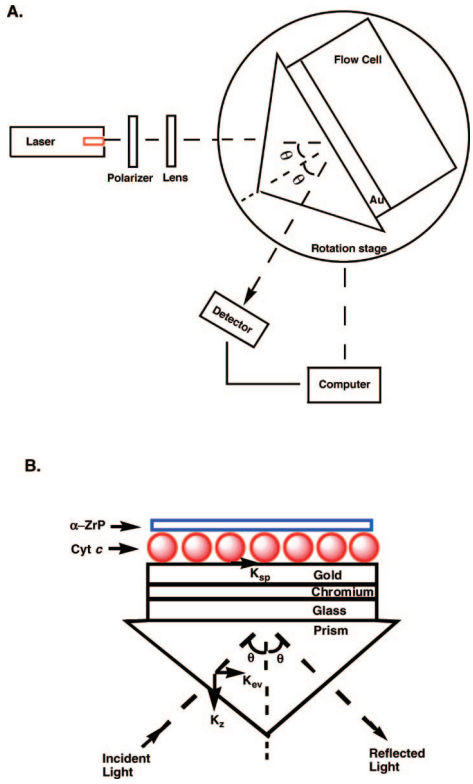

[a] Cyt *c* was self-assembled on the Au film, and exfoliated α-ZrP (or α-ZrCEP) particles were adsorbed onto the Cyt *c* layer. Urea solutions were flowed over the protein layer to monitor protein unfolding or refolding by SPR

K_2HPO_4 buffer, pH 7.2) with a step increment of 1M. In control experiments, the SAM formed by aminoethanethiol (AET) on Au was used instead of Cyt *c*, because AET structure is not influenced by urea and the adsorption of ZrP on AET SAM is known.[30] Angle-resolved SPR curves were obtained as a function of urea concentrations, in all cases, and data were analyzed by the following equations:[10]

$$\Delta(R_{min}/R_0) = f_N(\Delta(R_{min}/R_0)_N) + f_D(\Delta(R_{min}/R_0)_D) \quad (1)$$

$$K_{eq} = [D]_{eq}/[N]_{eq} = (f_D/f_N) = (f_D/(1-f_D)) \quad (2)$$

$$\Delta G^o = -RT\ln(K_{eq}) \quad (3)$$

$$\Delta G^o = \Delta G^o_{water} + k[\text{urea}] \quad (4)$$

In the above equations, $\Delta(R_{min}/R_0)_X$ is the change in reflectivity measured by SPR, f_x is the fraction of Cyt *c* with x being the folded, N, or unfolded, D, form of the protein, K_{eq} is the equilibrium constant, R is the gas constant, T is temperature (298 K), $\Delta G_{water}°$ is the intrinsic Gibbs free energy change, and k represents the propensity for unfolding by urea.

Electrochemical Studies. Square wave voltammetry (SWV) was carried out on Cyt *c*/Au in the presence and in the absence of urea. Au electrodes (2 mm diameter, CH Instruments) were cleaned by soaking in piranha solution for 10 min, followed by rinsing with deionized water, polishing for 2 min with 0.3 μm alumina slurry, and sonicating for 30 s in deionized water. This was followed by cycling in 0.5 M H_2SO_4 for 10 min from −0.2 to 1.65 V to obtain a reproducible, known cyclic voltammogram (CV) of the Au electrode. The area of the electrode was determined to be 0.05 (±0.02) cm^2 on the basis of Au oxide reduction wave integration upon scanning from 0 to 1.47 V in the acid solution.[27] After removal from the acid, the electrodes were immediately rinsed with absolute ethanol. For adsorption studies, the electrode was exposed directly to the Cyt *c* solution for 1 h at 4 °C. For bare electrode runs, the electrode was immediately placed into the electrochemical run buffer (10 mM KH_2PO_4 pH 7.2) to minimize any nonspecific adsorption of exogenous material. Square-wave voltammograms (5 Hz frequency, 25 mV pulse, and 4 mV step) were acquired by using a CH Instruments (Austin, TX) Model 660 potentiostat. A platinum counter electrode and a saturated calomel reference electrode (SCE) were employed for these measurements. Solutions were aggressively purged with purified N_2 for at least 15 min before each run, and N_2 atmosphere was maintained above the solution for the duration of the experiment.

Results and Discussion

SPR was used to quantify the free energy changes accompanying the unfolding of Cyt *c* at specific environments, and the data clearly demonstrate the sensitivity of SPR to protein conformation as well as the strong role of surface groups on protein stability.

α-ZrP/Cyt c/Au Assembly. First, Cyt *c* was adsorbed onto the Au film, and the corresponding angular-dependent SPR profiles were recorded (Figure 1A). These matched with those reported.[10] Time-resolved SPR signals (Figure 1B) indicated a rapid initial rise with a slope of 4.8×10^{-5} s^{-1} M^{-1}. This was followed by a much slower growth, on longer time scales. Next, Cyt *c*/Au assembly was exposed to a suspension of α-ZrP, and adsorption of α-ZrP on to the protein film was monitored in real time (Figure 1C).

Binding of the large particles of α-ZrP (~600 Å in diameter) to the protein layer was rather slow, and the initial slope of the linear fit to the data was 3.8×10^{-6} s^{-1} per molar α-ZrP. This rate constant is nearly an order of magnitude smaller than the rate constant for the binding of Cyt *c* to Au, and the decrease is consistent with the larger size of the α-ZrP platelets (600 nm diameter disks).[18] Note that these kinetic traces are the very first time-resolved measurements of the binding of any protein to these inorganic solids. These open new opportunities to examine the kinetics of protein binding to solids.

After α-ZrP binding saturated, excess solid washed away, and the SPR angular profile was recorded (Figure 1A, thick line). The minimum shifted from 64.8° for Cyt *c*/Au to 65.3° for α-ZrP/Cyt *c*/Au, and the shift to higher angles confirmed the adsorption of α-ZrP.

AFM Studies. The nanoassemblies were further characterized by AFM. Tapping-mode AFM images of Au, Cyt *c*/Au, and α-ZrP/Cyt *c*/Au are shown in Figure 2. Distinct changes in the surface morphology arising from the adsorption of Cyt *c* on Au were observed, and the AFM images were reproducible after repetitive scans or after thorough washing with buffer, as expected.[28] The Au surface used in our study has an average surface roughness of 1.164 nm (Figure 2A), and exposure of bare Au to Cyt *c* resulted in an increase in the surface roughness (1.915 nm, Figure 2B). These images showed a more globular morphology than bare gold, which is consistent with protein adsorption on Au.[28,29]

Exposure of α-ZrP to Cyt *c*/Au SAM further changed the surface morphology, and this demonstrated large sheet-like structures and ridges (Figure 2C). Formation of irregularly shaped, puckered α-ZrP sheets with distinct edges were also

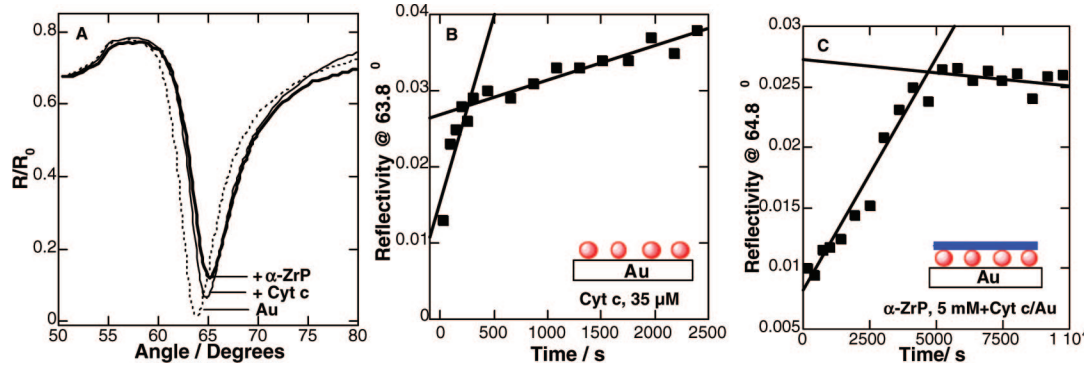

Figure 1. (A) Angle-resolved SPR profiles of bare Au (dashed line), Cyt *c*/Au (thin line), and α-ZrP/Cyt *c*/Au (thick line). The SPR minimum shifted from 63.8° for bare Au to 64.8° for Cyt *c*/Au to 65.3° for α-ZrP/Cyt *c*/Au. (B) Time-resolved SPR data for Cyt *c* binding to Au (at 63.8°). Solid lines are linear fits to the data. (C) Time-resolved SPR data for α-ZrP binding to Cyt *c*/Au (at 64.8°).

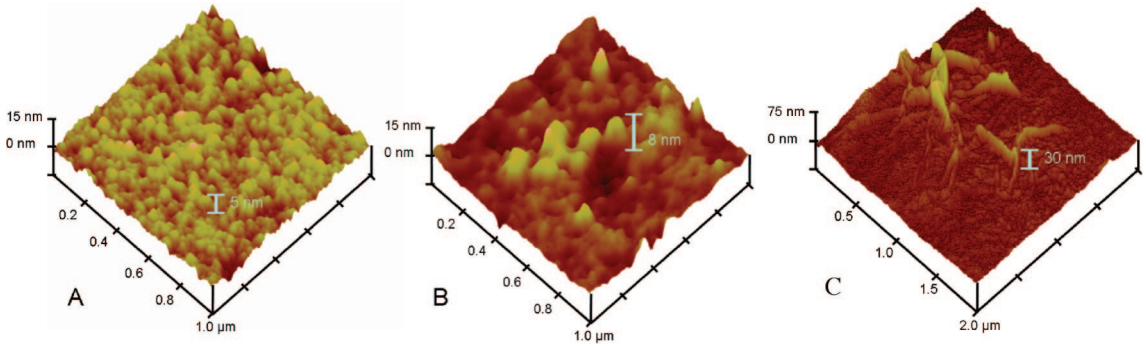

Figure 2. Tapping-mode AFM image of (A) bare Au (111), (B) Cyt *c* adsorbed on Au, and (C) α-ZrP adsorbed on Cyt *c*/Au. The Au slides were washed excessively with buffer and dried before acquiring the AFM images. A vertical bar of 15 nm with a scan area of 1 × 1 μm for bare Au and Cyt *c*/Au and a vertical bar of 75 nm with a scan area of 2 × 2 μm for α-ZrP/Cyt *c*/Au are shown.

observed by others.[30,30] This type of surface morphology explains the large film thickness observed here, where multiple layers of the inorganic particles adsorb on the protein. The AFM images demonstrate α-ZrP adsorption to the protein layer.

EDX Studies. The above samples were examined by EDX to ascertain the elemental compositions of the layers, and the data are consistent with AFM studies (Supporting Information, #2). After the self-assembly of Cyt *c* on Au, the wt% of C, N, O, and S are increased, whereas that of Au decreased. Similarly, the wt% of C, N, O, and S decreased, and that of Zr increased after the adsorption of α-ZrP on Cyt *c*/Au. Note that the EDX peaks of Zr and Au are too close to be well separated (Zr La1 = 2.042 keV, Au Ma1/2 = 2.12 keV), and the smaller than expected values for Zr is due to this overlap.

Reversible Protein Unfolding. The stability of α-ZrP/Cyt *c*/Au assembly was evaluated by exposure to increasing concentrations of urea (0−7 M). Urea is well-known to denature proteins, and SPR is known to be a very sensitive marker for protein conformational changes.[10–12] Therefore, SPR profiles of α-ZrP/Cyt *c*/Au were recorded with increasing urea concentrations (Figure 3A). The data indicate a progressive shift of the SPR minimum from 65.3° at 0 M urea to 71.3° at 7 M urea, as well as a decrease in the minimum reflectivity. These changes are consistent with urea-induced protein unfolding and the concomitant expansion of the polypeptide chain from the surface.[10–12]

Urea-induced SPR changes are completely reversible. At the end of the above treatment, the protein assembly was subjected to decreasing concentrations of urea from 7 to 0 M (Figure 3B). The changes, in terms of the position of the minimum and its depth, are completely reversible, and the curves recorded at 0 M urea before or after unfolding, from panels A and B, are superimposable. This finding is significant for two reasons: (1) protein unfolding is completely reversible and (2) the inorganic layer was retained during the entire process of urea-induced unfolding and refolding, and no permanent changes are noted.

Because the protein is covalently linked to the underlying Au film, the denatured protein was retained on the solid, and because the heme group in Cyt *c* is covalently linked to the peptide backbone, heme is not released. These factors facilitated the refolding of Cyt *c*. Even so, such reversible unfolding at a solid surface is surprising, and reversibility permits us to analyze the data by using equilibrium thermodynamics.

Electrochemical Studies. The protein assemblies were interrogated in electrochemical studies to evaluate the redox properties of Cyt *c* before and after unfolding. Because of its high sensitivity, SWV was used for this purpose (Figure 4).

These results demonstrate the electrochemical responses of bare Au (Figure 4, curve a) and Au coated with Cyt *c* (10 mM phosphate buffer pH 7.2) in the absence (Figure 4, curve b) or the presence (Figure 4, curve c) of 7 M Urea. The initial SWV for the Cyt *c*/Au electrode (Figure 4, curve b) shows a clear reduction wave at $E = -0.46$V versus SCE with a peak current (i_p) of 34 nA. The large negative potential shift from native Cyt *c* (12−50 mV versus SCE) was previously attributed to adoption of a non-native structure, as Cyt *c* becomes surface bound.[31–34] Adsorption alters heme axial ligand orientation, affecting the stability of the reduced heme, and shifts the reduction potential to approximately 400 mV negative (−360 to −460 mV versus SCE). This was demonstrated in the literature by using ligand exchange[35] and site-directed mutagenesis experiments.[32] The axial ligand exchange with water promotes a loose orientation of the heme pocket and increased

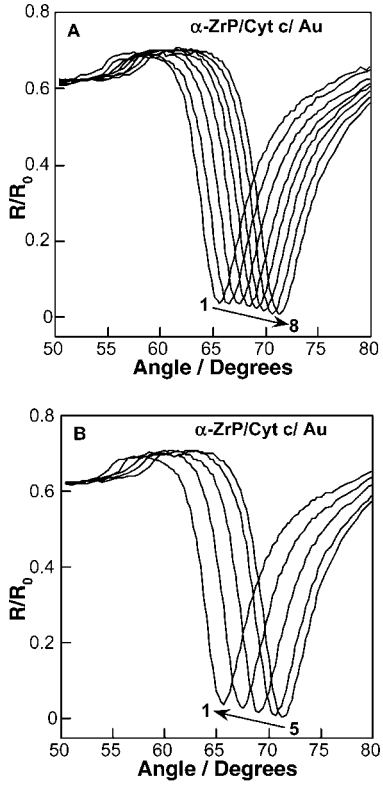

Figure 3. Angle-resolved SPR curves of α-ZrP/Cyt *c*/Au recorded as a function of urea concentration, (A) increasing urea concentration (0, 1, 2, 3, 4, 5, 6, and 7 M urea, curves 1−8, respectively) and (B) decreasing concentrations of urea (7, 6, 4, 2, and 0 M urea, curves 5−1, respectively). The curves corresponding to 0 M urea, before and after exposure to urea (panel B, curve 1 and panel C, curve 1) are completely superimposable.

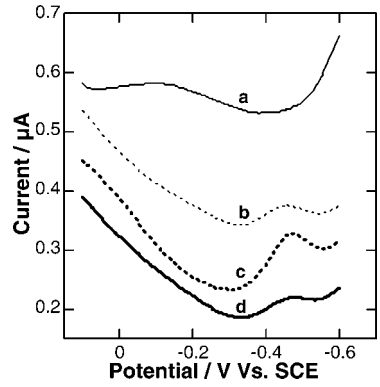

Figure 4. SWV of (a) bare Au, (b) Cyt *c*/Au, (c) Cyt *c*/Au in presence of 7 M urea, and (d) Cyt *c*/Au after washing off urea with 10 mM K_2HPO_4 pH 7.2. An increase in peak current is evident in the presence of urea. After removal of urea, the reduction wave profile matched with the initial SWV for Cyt *c*/Au, which indicates reversible unfolding.

solvent exposure resulting in decreased stability of the reduced form and large negative potential shifts.[33]

Upon exposure of the Cyt *c* coated electrode to 7 M urea, the reduction wave shifted negatively by an additional 10 mV ($E = -0.47$ V, Figure 4, curve c), and peak current increased in magnitude to 95 nA. The increase in peak current denotes further promotion of non-native Cyt *c* by urea, and the slightly negative potential shift is consistent with further extension of the more open oxidized form because of unfolding. Similar electrochemical results were seen upon altering the identity of Phe82, which serves to stabilize the heme environment.[32,36]

After removal of urea from the solution, in our experiments, the reduction wave returned to the initial values, $E = -0.46$ V and $i_p = 34$ nA (Figure 4, curve d). As seen in SPR studies, the electrochemical studies also support reversible protein unfolding by urea. The reduction waves presented here are not due to cysteine thiolate desorption, which occurs at approximately −0.8 V versus SCE at neutral pH.[34] Therefore, Cyt *c* remains covalently bound to the Au surface via Cys102 for the duration of the experiment, and the folding of the surface bound Cyt *c* is tunable by urea exposure. Results with bare Au electrode also demonstrate that the reduction wave at −0.46 V (Figure 4, curve b) is indeed due to Cyt *c*/Au and not to the phosphate buffer, urea, or other material bound to the electrode.

CVs were also done on Cyt *c*/Au electrodes to obtain surface coverage by integrating the reduction peaks at −0.46 V versus SCE for denatured Cyt *c* at scan rates of 10−100 mV s^{-1}. This gave a surface coverage of $9.11 \pm 0.22 \times 10^{-12}$ mol cm^{-2}, or 5.5×10^{12} molecules of Cyt *c* per cm^2. The peak for the denatured protein was used because we reasoned that this would give the best estimate of the total heme present from Cyt *c* on the surface. A close packed monolayer of Cyt *c* on Au provides[37] 1.44×10^{-11} mol cm^{-2}; therefore, the active protein coverage on the electrode is 63% of the total electrode area. This value is in reasonable agreement with the EDX data. With the electrochemical data supporting the redox activity of the bound protein and the reversible unfolding of Cyt *c* by urea, we next examined in control studies whether the urea-induced SPR changes are unique to the protein layer.

AET Assemblies. Control experiments were designed where Cyt *c* SAM was replaced by a positively charged, 2-aminoethane thiol (AET) SAM (Chart 2C). The AET/Au SAM was prepared, and α-ZrP was bound to it, as reported elsewhere.[30,30] The formation of both AET/Au and α-ZrP/AET/Au was monitored by time-resolved SPR as well as angle-resolved SPR (Figure 5A). The adsorption of AET to Au shifted the profile from 63.8° to 64.0°, and the adsorption of α-ZrP further increased the angle to 64.5°. The reflectivity minima decreased as adsorption progressed, and these changes support the formation of the nanoassemblies. Note that excess reagents were washed away before recording the SPR profiles.

From the time-resolved SPR studies, the rate constant for the adsorption of α-ZrP onto AET/Au layer is 7.4×10^{-5} s^{-1} per molar α-ZrP (data not shown), and this value is an order of magnitude greater than that observed for α-ZrP binding to Cyt *c*/Au. This increase in rate constant is consistent with the higher charge density expected for the AET/Au as compared to that of the Cyt *c*/Au.

The SPR resonance angle, the minimum reflectivity, and the full width at half minimum for the above SPR curves are compared (Supporting Information, #3). These data clearly show that the SPR curve corresponding to the adsorption of α-ZrP is similar in the two cases, and the minimum is shifted by 0.5° when α-ZrP binds to either AET/Au or Cyt *c*/Au. The minimum reflectivity values also changed from 97% for AET/Au to 88% for α-ZrP/AET/Au and from 92% for Cyt *c*/Au to 84% for α-ZrP/Cyt *c*/Au. The changes in the SPR angle (0.5°) and percent reflectivity (8.8% versus 8.3%) for the adsorption of α-ZrP on AET/Au versus Cyt *c*/Au are similar, as expected.

The exposure of α-ZrP/AET/Au to increasing concentrations of urea shifted SPR minima to higher angles (Figure 5B,C), but the minimum reflectivities did not change. The latter result is in contrast to the increase in the depth of the minimum noted with α-ZrP/Cyt *c*/Au. Increases in the depth of the SPR profiles of α-ZrP/Cyt *c*/Au, as a function of increasing urea concentra-

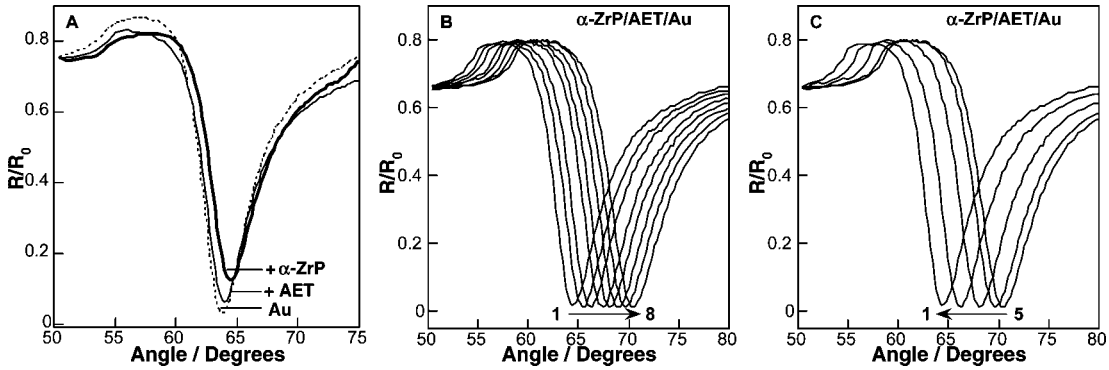

Figure 5. (A) SPR profiles of bare Au, AET/Au, and α-ZrP/AET/Au. (B). Angle-resolved SPR curves for α-ZrP/AET/Au as a function of increasing urea concentration (0, 1, 2, 3, 4, 5, 6, and 7 M, curves 1−8, respectively). (C) Angle-resolved SPR curves for α-ZrP/AET/Au as a function of decreasing urea concentration (7, 6, 4, 2, and 0 M urea, curves 5−1, respectively). The curves at 0 M urea, before and after exposure to urea (panel B, curve 1 and panel C, curve 1), are completely superimposable.

tion, is concomitant with the unfolding of the protein layer. Such changes in the SPR minima were previously reported for the urea or acid-induced unfolding of proteins.[10–12] Next, the influence of surface functions of the solid on the protein stability was examined by using α-ZrCEP in place of α-ZrP.

α-ZrCEP/Cyt c/Au Assemblies. Note that the OH group of α-ZrP is replaced by CH_2CH_2COOH groups in α-ZrCEP, and α-ZrCEP also binds a number of proteins under benign, ambient conditions. Therefore, this solid provides an interesting opportunity to examine the influence of surface groups on bound-protein stability.

The α-ZrCEP/Cyt *c*/Au assembly was constructed by following the same method as that for α-ZrP/Cyt *c*/Au, and adsorption of the solid was monitored by SPR. For example, the SPR profile shifted to higher angles as the adsorption of α-ZrCEP to Cyt *c*/Au continued and reached a plateau after several hours. α-ZrCEP/Cyt *c*/Au assembly is subjected to urea-induced unfolding while monitoring by SPR (Figure 6). As noted earlier, the SPR minimum shifted to higher angles, and the minimum intensity decreased with increased urea concentration. Upon washing the sample with buffer (no urea), the SPR curve was restored to the profile recorded at 0 M urea. Note that these urea-induced changes are similar to those observed with α-ZrP/Cyt *c*/Au.

In control experiments, α-ZrCEP/AET/Au assemblies were prepared, and urea treatment of these α-ZrCEP/AET/Au assemblies indicated shifting of the SPR profiles to higher angles (Figure 6B) but no change in the SPR minimum intensity noted. These data are similar to those observed for α-ZrP/AET/Au (Figure 5C), and the intensity changes at the SPR minimum are due to the protein but are not specific to the inorganic solid. Note that other studies also reported that protein unfolding resulted in similar decreases in the SPR minima.[10–12,38] These SPR changes are characteristic of protein conformational dynamics, and we use these changes to quantify unfolding free energy of Cyt *c* sandwiched between α-ZrP or α-ZrCEP and Au.

Thermodynamics of Unfolding. Urea-induced reversible denaturation of Cyt *c* in the solution phase was reported previously,[10,39,40] and we assume that equilibrium is established at each urea concentration in the inorganic nanoassemblies. This assumption is supported by the fact that the SPR curves recorded before and after urea treatment are superimposable. This is also confirmed by the electrochemical data, as discussed above. Because urea-induced changes are reversible, the thermodynamic treatment is appropriate. Note that the free energy difference between the initial and final states are measured in the current

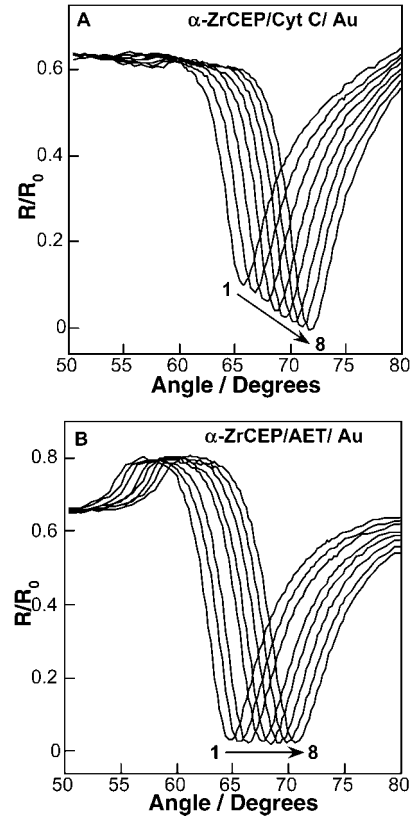

Figure 6. Angle-resolved SPR curves as a function of urea concentration (0, 1, 2, 3, 4, 5, 6, and 7 M urea, curves 1−8, respectively) of (A) α-ZrCEP/Cyt *c*/Au and (B) α-ZrCEP/AET/Au. A rapid increase in the depth of the SPR profile, as a function of urea concentration, is noted only for the sample containing the protein.

studies, and both states involve Cyt *c* bound to the solid. Therefore, the measured $\Delta G°$ values take into account the free energy contributions due to protein−solid interactions in both states.

From the SPR data showed in Figure 3, the ratio of the relative minimum reflectivity (R_{min}/R_0) at each urea concentration was normalized with respect to R_{min}/R_0 in the absence of urea, and these values have been plotted as a function of urea concentration (Figure 7A). The relative minimum reflectivity curves for Cyt *c*/Au (closed circles) and α-ZrP/Cyt *c*/Au (open squares) show a clear decrease in this ratio as the urea concentration increases. In contrast, the corresponding data for α-ZrP/AET/Au (crossed squares) show no significant changes under similar urea concentrations.

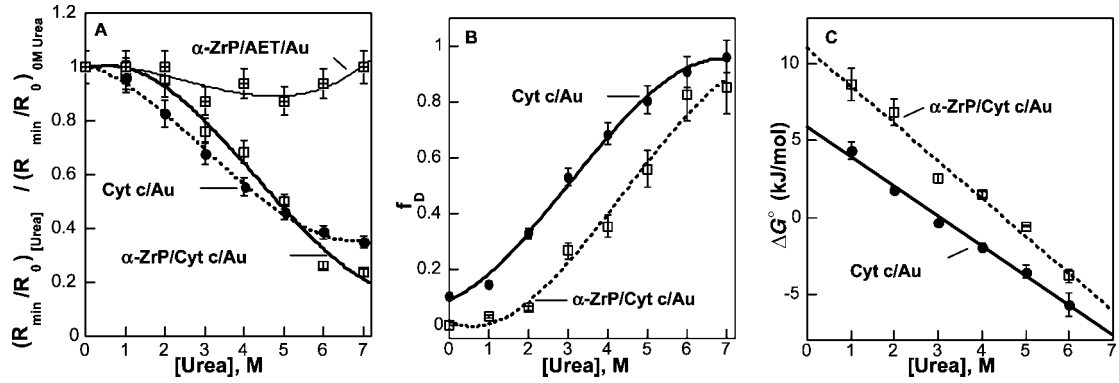

Figure 7. (A) Relative reflectivity profiles for Cyt *c*/Au (filled circles), α-ZrP/Cyt *c*/Au (open squares), and α-ZrP/AET/Au (crossed squares) as a function of urea concentration (0−7 M). The solid lines are smooth lines to guide the eye. (B) The fraction of protein unfolded as a function of urea concentration (0−7 M) for Cyt *c*/Au (filled circles) and α-ZrP/Cyt *c*/Au (open squares). (C) Plot of $\Delta G°$ (kJ/mol) as a function of urea concentration (0−7 M) for Cyt *c*/Au (filled circles) and α-ZrP/Cyt *c*/Au (open squares). The solid lines are linear fits to the experimental data.

TABLE 1: $\Delta G°$ Values for the Unfolding of Cyt *c* Bound to Au, in the Presence and Absence of α-ZrP or α-ZrCEP (in 10 mM K_2HPO_4 Buffer, pH 7.2) and $\Delta G°$ Value for Cyt *c* in Solution

sample	$\Delta G°$ (kJ/mol)	reference
Cyt *c*	26.8	refs 10, 42
Cyt *c*/Au	6.3 ±0.8	ref 10
α-ZrP/Cyt *c*/Au	10.9 ±1.3	this work
α-ZrCEP/Cyt *c*/Au	4.8 ±0.3	this work

Following eq 1, the SPR data for Cyt *c*/Au and α-ZrP/Cyt *c*/Au were used to plot the fraction of protein unfolded (*f*) as a function of urea concentration. These plots (Figure 7B) indicate that the protein in the assemblies is gradually unfolded by urea. The Cyt *c*/Au, however, responded initially to urea more quickly than α-ZrP/Cyt *c*/Au, which implies that the protein sandwiched between Au film and the inorganic layer shows a considerably greater resistance to unfolding than the protein on the Au film. One possible explanation is that the sandwich structure formed by the interactions between the protein, the Au film, and the inorganic layer restricts the protein to a pseudo-two-dimensional space. Such confinement is expected to decrease the entropy of unfolding and raise the stability of the confined protein.[41]

The data in Figure 7B are converted to a plot of ΔG^0 of unfolding versus urea concentration (Figure 7C), and the free energy change is estimated from the *y*-intercept. These values for Cyt *c*/Au and α-ZrP/Cyt *c*/Au are summarized in Table 1. The stability of Cyt *c*/Au is in good agreement with our earlier result, which was interpreted to show that the protein bound to the bare Au surface is less stable than that in solution. On the other hand, adsorption of α-ZrP layer improved protein stability by more than 4 kJ/mol. It is important to note that sandwiched Cyt *c* is still less stable than free protein in solution, but the current approach provides a simple route to enhance the thermodynamic stability of Cyt *c* layers. Two distinct contributions to this improved stability may be anticipated: mechanical confinement between the layers and stabilization via specific interactions with the inorganic solid. These aspects are further tested with α-ZrCEP/Cyt *c*/Au assemblies.

The above analysis of α-ZrCEP/Cyt *c*/Au data indicated a $\Delta G°$ of 4.8 ± 0.3 kJ/mol (Table 1), which is substantially less than that of α-ZrP/Cyt *c*/Au (10.9 ± 1.3 kJ/mol). Current data are consistent with our previous studies which showed that Cyt *c*/α-ZrCEP unfolded around 53 °C, whereas Cyt *c*/α-ZrP retained a substantial fraction of the native structure even at 89 °C.[20] Taken together, these studies indicate that SPR can serve as a sensitive noncalorimetric method to quantify the thermodynamic stabilities of proteins bound to solid surfaces.

Because both these inorganic solids can provide mechanical constraints to protein unfolding in the assemblies, the differences in the $\Delta G°$ values are likely due to the differences in the types of interactions that the surface groups can support. As pointed out earlier, α-ZrP differs from α-ZrCEP in terms of the surface functional groups (OH versus COOH). The hydroxyl functions of α-ZrP engage in intralayer hydrogen bonding rather than interlayer hydrogen bonding.[43] Therefore, this solid is unlikely to support hydrogen bonding with the bound protein.

On the contrary, interlayer hydrogen bonding between the carboxyl functions of α-ZrCEP is known;[44] hence, these could hydrogen-bond with the bound protein and distort the protein structure, lowering its stability. This is very likely the reason for the observed differences between the two solids, and SPR is an excellent method to probe protein−solid interactions on a quantitative basis.

Conclusions

The strategy described here enables the study of protein adsorption at a variety of solid surfaces in real time by SPR, and SPR is a sensitive, noncalorimetric method to quantify bound-protein stability. Sensitivity of SPR to protein conformational changes is now well established in the literature, and this lends support to the current approach to extend the studies to protein unfolding.[10–12] Urea-induced unfolding, as indicated by SPR, is also confirmed by the electrochemical data, and upon urea removal, the SPR profiles (Figures 3 and 6), as well as the voltamograms, returned to their initial values (Figure 4). Therefore, unfolding is reversible at all the surfaces examined here.

The unfolding free energy strongly depended on the characteristics of the solid in contact with Cyt *c*. α-ZrP enhanced protein stability by a substantial amount, from 6.3 to 10.9 kJ/mol, whereas α-ZrCEP destabilized it from 6.3 to 4.8 kJ/mol. The large difference in the protein stabilities between these two solids (6.1 kJ/mol) is likely due to the differences in terms of their surface groups (OH versus COOH). The data clearly demonstrate the utility of SPR to evaluate the role of specific surface groups on protein stability. It should be noted that the protein layer is in contact with the inorganic solid on one side and the underlying Au layer on the other side. Therefore, the values reflect the interactions with the inorganic solid as well as the Au layer.

Our strategy can be used essentially with any solid material that interacts with the protein layer and any protein which can be anchored onto the Au film, directly or indirectly. The data

thus obtained might form a framework for engineering more effective biomaterials for biosensing and biocatalysis.

Acknowledgment. C.V.K. thanks the National Science Foundation (DMR-0300631, DMR-0604815) for the financial support of this work. Participation of J.F.R., G.J., and E.G.H. was supported by US PHS Grants no. ES013557 and no. ES03154 from the National Institute of Environmental Health Sciences (NIEHS), NIH, USA. This paper is dedicated to the fond memory of Professor John Stock.

Supporting Information Available: X-ray photoelectron spectrum of Cyt *c* adsorbed on the Au film (#1); Energy dispersive X-ray absorption (EDX) data for Au, Cyt *c*/Au, and α-ZrP/Cyt *c*/Au samples (#2); and SPR trough position, depth, and full width at half minima (#3). This material is available free of charge via the Internet at http://pubs.acs.org.

References and Notes

(1) Torchilin, V. P. *Progress in Clinical Biochemistry and Medicine: Immobilized Enzymes in Medicine*; Springer-Verlag: Berlin 1991, Vol. 11, pp 206.

(2) (a) Gubitz, G.; Kunssberg, E.; van Zoonen, P.; Jansen, H.; Gooijer, C.; Velthorst, N. H.; Fei, R. W. In *Chemically Modified Surfaces*; Leyden, D. E., Collins, W. T., Eds.; Gordon and Breach: London, 1988; Vol. 2, pp 129. (b) Gorton, L.; Marko-Varga, G.; Dominguez, E.; Emneus, J. In *Analytical Applications of Immobilized Enzyme Reactors*; Lam, S., Malikin, G., Eds.; Blackie Academic & Professional: New York, 1994; pp 51.

(3) (a) *Biosensors in Analytical Biotechnology*; Freitag, R., Ed.; Academic Press: San Diego, 1996. (b) Rosevear, A.; Kennedy, J. F.; Cabral, J. M. S. *Immobilized Enzymes and Cells*; Adam Hilger: Philadelphia 1987; pp 248.

(4) (a) Niehaus, F.; Bertoldo, C.; Kähler, M.; Antranikian, G. *Appl. Microbiol. Biotechnol.* **1999**, *51*, 711. (b) Blair, E.; Greaves, J.; Farmer, P. J. *J. Am. Chem. Soc.* **2004**, *126*, 8632. (c) Fitter, J.; Haber-Pohlmeier, S. *Biochemistry* **2004**, *43*, 9589.

(5) (a) Bokhari, S. A.; Afzal, A. J.; Rashid, H. H.; Rojaka, M. I.; Siddiqui, K. S. *Biotechnol. Prog.* **2002**, *18*, 276. (b) Gonzalez-Blasco, G.; Sanz-Aparicio, J.; Gonzalez, B.; Hermoso, J. A.; Polaina, J. *J. Biol. Chem.* **2000**, *275*, 13708. (c) Reading, N. S.; Aust, S. D. *Biotechnol. Prog.* **2000**, *20*, 326. (d) Joe, K.; Borgford, T. J.; Bennet, A. J. *Biochemistry* **2004**, *43*, 7672.

(6) Pessela, C. C.; Mateo, C.; Fuentes, M.; Vain, A.; Garcia, J. L.; Carrascosa, A. V.; Guisan, J. M.; Fernandez-Lafluente, R. *Biotechnol. Prog.* **2004**, *20*, 388.

(7) Klein, M. D. *Trends Biotechnol.* **1986**, *4*, 179.

(8) Watanabe, S.; Shimizu, Y.; Teramatsu, T.; Murachi, T.; Hino, T. *Methods Enzymol.* **1988**, *137*, 54.

(9) Kim, J.; Jia, H.; Wang, P. *Biotechnol. Adv.* **2006**, *24*, 296.

(10) Chah, S.; Kumar, C. V.; Hammond, M. R.; Zare, R. N. *Anal. Chem.* **2004**, *76*, 2112.

(11) (a) Winzor, D. *Anal. Biochem.* **2003**, *318*, 1–12. (b) Tassiusa, C.; Moskalenkoa, C.; Minardb, P.; Desmadrilb, M.; Elezgarayc, J.; Argoula, F. *Physica A* **2004**, 342–402. (c) Yamaguchi, S.; Mannen, T.; Zako, T.; Kamiya, N.; Nagamune, T. *Biotechnol. Prog.* **2003**, *19*, 1348. (d) Chah, S.; Hammond, M. R.; Zare, R. N. *Chem. Biol.* **2005**, *12*, 323–328.

(12) (a) Jones, D. B.; Hutchinson, M. H.; Middelberg, A. P. J. *Proteomics* **2004**, *4*, 1007. (b) Xiang, J.; Guo, J.; Zhou, F. *Anal. Chem.* **2006**, *78*, 1418–1424. (c) Kang, T.; Hong, S.; Choi, I.; Sung, J. J.; Kim, Y.; Hahn, J.-S.; Yi, J. *J. Am. Chem. Soc.* **2006**, *128*, 12870–12878.

(13) (a) Kumar, C. V.; McLendon, G. L. *Chem. Mater.* **1997**, *9*, 863. (b) Kumar, C. V.; Chaudhari, A. *J. Am. Chem. Soc.* **2000**, *122*, 830.

(14) (a) Kumar, C. V.; Chaudhari, A. *Chem. Mater.* **2000**, *13*, 236. (b) Kumar, C. V.; Chaudhari, A. *Microporous Mesoporous Mater.* **2001**, *47*, 407.

(15) Bhambhani, A.; Kumar, C. V. *Adv. Mater.* **2006**, *18*, 239.

(16) (a) Kumar, C. V.; Chaudhari, A. *J. Am. Chem. Soc.* **1994**, *116*, 403. (b) Kumar, C. V.; Chaudhari, A. *Microporous Mesoporous Mater.* **2000**, *41*, 307.

(17) (a) Kumar, C. V.; Chaudhari, A. *Chem. Commun.* **2002**, 2382. (b) Kumar, C. V.; Chaudhari, A. *Microporous Mesoporous Mater.* **1999**, *32*, 75.

(18) Kumar, C. V.; Chaudhari, A. *Microporous Mesoporous Mater.* **2002**, *57*, 181.

(19) Chaudhari, A.; Thota, J.; Kumar, C. V. *Microporous Mesoporous Mater.* **2004**, *75*, 281.

(20) Chaudhari, A.; Kumar, C. V. *Microporous Mesoporous Mater.* **2005**, *77*, 175.

(21) Jagannadham, V.; Bhambhani, A.; Kumar, C. V. *Microporous Mesoporous Mater.* **2006**, *88*, 275.

(22) Bhambhani, A.; Kumar, C. V. *Chem. Mater.* **2006**, *18*, 740.

(23) Panchagnula, V.; Kumar, C. V.; Rusling, J. F. *J. Am. Chem. Soc.* **2002**, *124*, 12515.

(24) Bhambhani, A.; Kumar, C. V. *Chem. Mater.* **2008**, *109*, 223.

(25) Andersen, J. E. T.; Møller, P.; Pedersen, M. V.; Ulstrup, J. *Surf. Sci.* **1995**, *325*, 193.

(26) (a) Alberti, G.; Costantino, U. In *Intercalation Chemistry*; Whittingham, M. S., ; Jacobson, A. J.; Eds.; Academic Press Inc.: NY, 1982; Chapter 5. (b) Alberti, G.; Costantino, U.; Giulietti, R. *J. Inorg. Nucl. Chem.* **1980**, *42*, 1062. (c) Dines, M. B.; DiGiacomo, P. M. *Inorg. Chem.* **1981**, *20*, 92.

(27) Bard, A. J.; Faulkner, L. R. *Electrochemical Methods: Fundamentals and Applications*; 2nd ed., John Wiley and Sons: New York, 2001.

(28) Bonanni, B.; Alliata, D.; Bizzari, A. R.; Cannistraro, S. *Chem. Phys. Chem.* **2003**, *4*, 1183.

(29) Louie, G. V.; Brayer, G. D. *J. Mol. Biol.* **1990**, *214*, 527.

(30) Fang, M.; Kaschak, D. M.; Sutorik, A. C.; Mallouk, T. E. *J. Am. Chem. Soc.* **1997**, *119*, 12184.

(31) Komar-Panicucci, S.; Weis, D.; Bakker, G.; Quio, T.; Sherman, F.; McLendon, G. *Biochemistry* **1994**, *33*, 10556.

(32) Feinberg, B. A.; Liu, X.; Ryan, M. D.; Schejter, A.; Zhang, C.; Margoliash, E. *Biochemistry* **1998**, *37*, 13091.

(33) Texcan, F. A.; Winkler, J. R.; Gray, H. B. *J. Am. Chem. Soc.* **1998**, *120*, 13383.

(34) Hansen, A. G.; Boisen, A.; Neilsen, J. U.; Wackerbarth, H.; Chorkendorff, I.; Andersen, J. E. T.; Zhang, J.; Ulstrup, J. *Langmuir* **2003**, *19*, 3419.

(35) Battistuzzi, G.; Borsari, M.; Cowan, J. A.; Ranieri, A.; Sola, M. *J. Am. Chem. Soc.* **2002**, *124*, 5313.

(36) Pearce, L. L.; Gartner, A. L.; Smith, M.; Mauk, A. G. *Biochemistry* **1989**, 3152.

(37) Sagara, T.; Niwa, K.; Sone, A.; Hinnen, C.; Niki, K. *Langmuir* **1990**, *6*, 254–262.

(38) We also examined by SPR the urea-induced unfolding of Cyt *c* covalently bound to a SAM similar to AET/Au but terminated with hydroxyl functions. Preliminary data show that a similar shift in the SPR minima to higher angles and changes in the depth of the minima are noted. The unfolding free energy calculated by the procedure described in this article was found to be 8.8 ± 1.0 kJ/mol.

(39) Gupta, R.; Ahmad, F. *Biochemistry* **1999**, *38*, 2471.

(40) Gianni, S.; Brunori, M.; Travaglini-Allocatelli, C. *Protein Sci.* **2001**, *10*, 1685.

(41) Zhou, H.-X.; Dill, K. A. *Biochemistry* **2001**, *40*, 11289.

(42) Huyghues-Despointes, B. M. P.; Scholtz, J. M.; Pace, C. N. *Nat. Struct. Biol.* **1999**, *6*, 910.

(43) Kumar, C. V.; Bhambhani, A.; Hnatiuk, N. In *Handbook of Layered Materials*; Carrado, K., Dutta, P.; Auerbach, S., Eds.; Marcel Dekker: NY, 2004; Vol. 2, pp 313.

(44) (a) Burwell, D. A.; Thompson, M. E. *Chem. Mater.* **1991**, *3*, 730. (b) Burwell, D. A.; Valentine, K. G.; Timmermans, J. H.; Thompson, M. E. *J. Am. Chem. Soc.* **1992**, *114*, 4144.

JP7121642